Physics of Fluids

Modeling the evaporation of sessile drops deformed by gravity on hydrophilic and hydrophobic substrates

Cite as: Phys. Fluids **35**, 032113 (2023); https://doi.org/10.1063/5.0143575
Submitted: 24 January 2023 • Accepted: 26 February 2023 • Published Online: 16 March 2023

S. Tonini and G. E. Cossali

Physics of Fluids ARTICLE scitation.org/journal/phf

Modeling the evaporation of sessile drops deformed by gravity on hydrophilic and hydrophobic substrates

Cite as: Phys. Fluids **35**, 032113 (2023); doi: 10.1063/5.0143575
Submitted: 24 January 2023 · Accepted: 26 February 2023 ·
Published Online: 16 March 2023

View Online Export Citation CrossMark

S. Tonini[a] and G. E. Cossali

AFFILIATIONS

Department of Engineering and Applied Sciences, University of Bergamo, Viale Marconi 5, 24044 Dalmine, Bergamo, Italy

[a]Author to whom correspondence should be addressed: simona.tonini@unibg.it

ABSTRACT

Evaporation of sessile drops deformed by gravity is quantified by an analytical–numerical approach. The shape of the drops is defined by minimizing the interfacial and potential drop energies, following a variational integral approach, for a wide range of drop sizes (from 2.7 μl to 1.4 ml for water drops) and contact angles for both hydrophilic and hydrophobic substrates. The extension of an analytical model for drop evaporation, which accounts for the effect of the Stefan flow and the temperature dependence of thermophysical properties, to the present conditions reduces the problem to the solution of a Laplace equation, which is then numerically calculated using COMSOL Multiphysics®. The vapor fluxes and evaporation rates are then quantified, and the systematic approach to the problem allows the derivation of two correlations, for hydrophilic and hydrophobic substrates, respectively, that can be used to correct the evaporation rate calculated for a drop of the same volume and contact angle in the absence of gravity effects.

NOMENCLATURE

A	Non-dimensional function [Eq. (4)] (-)
a_k, b_k, c_k	Non-dimensional coefficients (-)
Bo	Bond number, $Bo = \frac{\rho g R_{eq}^2}{\sigma}$ (-)
c	Molar density (kg/kmol)
C_j	Non-dimensional coefficients (-)
D_{10}	Mass diffusion coefficient (m^2/s)
f	Non-dimensional function [Eq. (3)]
g	Gravitational acceleration (m^2/s)
G	Correction factor, $G = \frac{m_{ev}(R_{eq},\theta_c,\lambda^*)}{m_{ev}(R_{eq},\theta_c,0)}$ (-)
H	Logarithm of gas molar fraction, $H = \ln(y^{(0)})$ (-)
K_G	Gaussian curvature (m^{-2})
K_G^*	Non-dimensional Gaussian curvature: $\hat{K}_{G,ses} = \sqrt{2}(R_{eq}^2 K_G)$ (-)
L_c	Capillary length, $L_c = (\frac{\sigma}{\rho g})^{1/2}$ (m)
m_{ev}	Evaporation rate (kg/s)
M_m	Molar mass (kg/kmol)
$n_j^{(p)}$	Mass flux of species (p) (kg/m^{2}s)
$N_j^{(p)}$	Molar flux of species (p) (kmol/m^{2}s)
r	Radial cylindrical coordinate (m)
R	Radial distance from the origin (m)
R_c	Base radius of the spherical cap (m)
R_d	Spherical cap radius (m)
R_{eq}	Equivalent drop radius (m)
S	Drop surface area (m^2)
t	Non-dimensional parameter (-)
V	Volume (m^3)
W	Scaling parameter (m)
$y^{(p)}$	Molar fraction (-)
z	Axial cylindrical coordinate (m)

Greek symbols

α	Non-dimensional shape function (-)
θ_c	Contact angle (°)
λ	Non-dimensional constant in Eq. (4), $\lambda = \frac{g\rho w^2}{\sigma}$ (-)
ρ	Mass density (kg/m^3)
σ	Surface tension (kg/s^2)
Φ	Harmonic auxiliary function (-)
ϕ	Polar angle (°)

Subscripts

ev	Evaporation

max	Maximum
min	Minimum
n	Orthogonal to drop surface
ob	Oblate
s	Drop surface
ses	Sessile
∞	Ambient conditions

Superscripts

T	Total
ˆ	Non-dimensional

Abbreviations

LHS	Left-hand side
RHS	Right-hand side

I. INTRODUCTION

Evaporation of a sessile liquid drop gently deposed on a solid substrate is a phenomenon of enduring scientific interest, motivated by the complexity of the physical aspects involved, such as the drop shape, contact line instabilities, substrate thermal effects, and particle suspension, and its wide range of civil and industrial applications, from cooling technologies and DNA/RNA synthesis to ink-jet printing and pesticide spraying (refer to Refs. 1–3 for recent reviews on the extensive experimental, numerical, and analytical work done on the topic of sessile drop evaporation).

In analytical approaches to the modeling of drop evaporation, quasi-steadiness is often assumed, motivated by the time scales of mass and energy transport being orders of magnitude smaller than the drop lifetime, and in the absence of external convective flow, the evaporation of a liquid sessile drop can be described as a diffusion-limited process. Under the further assumption of constant thermophysical properties of the gas mixture, the analytical description of the problem reduces to the solution to the Laplace equation.[4] Recently, this last assumption was relieved, and an analytical solution to the species and energy conservation equations for a mono-component liquid sessile drop deposed on hydrophilic and hydrophobic substrates was proposed in Ref. 5, extending a model previously developed for suspended drops.[6]

Many other analytical approaches are available in the literature [refer to Refs. 3 and 7 for extensive reviews], and, except for the case of thin films, these models assume that the drop cap has a perfectly spherical shape, which is considered a reasonable assumption in the case of a drop size being smaller than the capillary length ($L_c = (\frac{\sigma}{g\rho})^{1/2}$). However, this becomes questionable for larger drops, when the effect of gravity is not negligible.

The first attempt to determine the shape of a sessile drop on a flat plate under the action of gravity and surface tension was likely that of Bashforth and Adams.[9] They derived a second-order non-linear differential equation for the drop shape in Cartesian coordinates. Robertson and Lehman[10] proposed a variational approach based on the minimization of the surface and potential energies of the drop on a flat plate, and a solution in the integral form was proposed to yield a more efficient numerical approach. In Ref. 11, it was observed that the value of the contact angle was not explicitly taken into account in the previous approach and a similar variational method was then proposed, taking into account also the liquid–solid and gas–solid contact energies, yielding the contact angle as a natural condition. Bormashenko and Whyman[12] showed that a similar approach could also be used for drops in force fields other than the gravitational, such as those due to centrifugation or electrical fields. The resulting differential equation generalizes the kind of potential that can be taken into account.

A few numerical works[16,17] recently appeared to account for the effect of drop shape on evaporation from a non-spherical sessile drop, analyzing how the liquid internal motion affects the heat and mass transfer. The effect of drop deformation induced by gravity on the evaporation of liquid drops deposited on horizontal and inclined surfaces has been numerically and analytically investigated in Ref. 18, expressing the drop shape as perturbation expansions in terms of the Bond number. The results showed a modest effect of drop deformation on the evaporation rate of drops on hydrophilic substrates, almost independently of the surface inclination.

The growing interest in the effect of drop deformation on evaporation is witnessed also by many studies that appeared in the recent literature (see, for example, Refs. 13–15 and references therein), showing the relevance of the research on this particular effect.

In the present work, a systematic study on the evaporation of sessile drops on hydrophilic and hydrophobic substrates accounting for the effect of gravity on the drop shape is proposed. The drop shape has been numerically defined minimizing the interfacial and potential drop energies following the method of Ref. 10. The vapor distribution around the drop was calculated by solving the conservation equations using COMSOL Multiphysics. This allows the quantification of the effect of drop deformation due to gravity on the drop evaporation rate. A correction to the Picknett–Bexon correlation[8] is proposed for drops on hydrophilic and hydrophobic substrates, varying the contact angle from 40° up to 150°, and with the Bond number, based on the equivalent volume radius, up to 30.

II. MATHEMATICAL MODELING

The present study focuses on the theoretical evaluation of the effect of the deformation due to gravity on the evaporation characteristic of a single component sessile drop on hydrophilic and hydrophobic substrates. External convection is neglected, except for the Stefan flow taken into account. Surface temperature is assumed uniform, and consequently, the molar fraction of the vapor in the gas mixture is assumed uniform over the drop surface. The case in the absence of gravity, when the drop assumes the form of a spherical cap, has been extensively studied under these simplifying assumptions, as reported above. In Ref. 8, Picknett and Bexon proposed a correction factor for the evaporation rate of a sessile drop as a function of the contact angle, with the assumption that the drop shape is that of a spherical cap.

As briefly summarized in Sec. I, the problem of determining the shape of a sessile drop subject to gravity has been extensively studied, since early work of Ref. 9, with different approaches. Here, the variational approach proposed by Ref. 10 will be used since the proposed integral solution was shown to be easily implementable for the numeric calculation of the drop shape.

The method to determine the shape is by minimizing the total energy, the sum of the interfacial energy, and the potential energy in the gravitation field, while maintaining constant the drop volume.

Following Ref. 10, let the drop profile in cylindrical coordinates be defined by

$$r = w\sqrt{1-t^2}, \tag{1}$$

$$z = w\alpha(t), \tag{2}$$

where t is a parameter going from t_0 (defined by $R_c = w\sqrt{1-t_0^2}$, where R_c is the drop base radius, see Fig. 1) to 1 (where $r=0$); $\alpha(t)$ is the function to find through the above-mentioned minimization and w is a scale factor.

The integral solution proposed in Ref. 10 is described by the following equations:

$$f(t) = \frac{1 - t^2 A(t)}{\sqrt{1 + (1-t^2)A(t)(2 - t^2 A(t))}}, \tag{3}$$

$$A(t) = \frac{\lambda}{2}\left\{\frac{1}{t^2}\int_0^t \xi^2 f(\xi)d\xi + \frac{1}{1-t^2}\int_t^1 (1-\xi^2) f(\xi)d\xi\right\}, \tag{4}$$

where $\lambda = \frac{g\rho w^2}{\sigma}$ and $\alpha(t) = \int_{t_0}^t f(\xi)d\xi$. To note that t_0 is negative when the substrate is hydrophobic (and positive for hydrophilic substrate); in fact,

$$\left(\frac{dz}{dr}\right)_{t=t_0} = -\frac{\sqrt{1-t_0^2} f(t_0)}{t_0}, \tag{5}$$

the function $f(t)$ must always be positive for $t > t_0$; since $\alpha = \frac{z}{w}$ must be positive, then the sign of the derivative of the profile on the wall is opposite to that of t_0. The contact angle is defined as

$$\theta_c = \pi - \arctan\left(-\frac{\sqrt{1-t_0^2} f(t_0, \lambda)}{t_0}\right). \tag{6}$$

The solution can be found by iterative substitution, using as a first guess $f = 1$ (circular profile), calculating $A(t)$ by numerical integration [Eq. (4)] and then finding the new guess for f [Eq. (4)]. Further iterations are needed to determine the value of t_0 for the given contact angle. Figure 2 shows a summary of the results. The function f is reported for values of λ ranging from 0 to 10 as solid curves. The dashed lines correspond to the given values of the contact angle and define the values of t_0 via the intersection with the solid curves.

The solution was compared with the numerical solution obtained by applying a Runge–Kutta method to the second order ordinary differential equation (ODE) that describes the drop profile, with very good agreement.

In the subsequent part of this study, the parameter $Bo = \frac{\rho g R_{eq}^2}{\sigma}$ will be used instead of λ since the volume equivalent radius, $R_{eq} = \left(\frac{V3}{4\pi}\right)^{1/3}$, is a direct measure of the drop volume.

Diffusion-limited models are used to describe the heat and mass transfer in the gas mixture surrounding a sessile drop since the vapor transport from the droplet into the surrounding mixture is the rate-limiting mechanism. For low and mild evaporation conditions, such as those usually describing sessile drop evaporation at moderate temperatures, quasi-steadiness can be safely assumed, and the transport phenomena can be modeled by the steady-state energy and species conservation equations.

For the single component drop, where the gaseous phase is a binary mixture of the evaporating species (vapor) and the ambient gas, the molar fluxes are

$$N_j^{(p)} = N_j^{(T)} y^{(p)} - cD_{10}\nabla_j y^{(p)}, \tag{7}$$

where c is the molar gas density, D_{10} is the binary mass diffusion coefficient, $y^{(p)}$ is the molar fraction of species p ($p = 0$ for the ambient gas, and $p = 1$ for the evaporating component), and

$$\nabla_j N_j^{(p)} = 0 \quad (p = 0, 1) \tag{8}$$

are the steady-state species conservation equations. Assuming that the ambient gas absorption into the liquid can be neglected, the quasi-steadiness assumption implies a still drop surface. Consequently, the flux of ambient gas, $N^{(0)}$, is nil on the surface, and, in the absence of

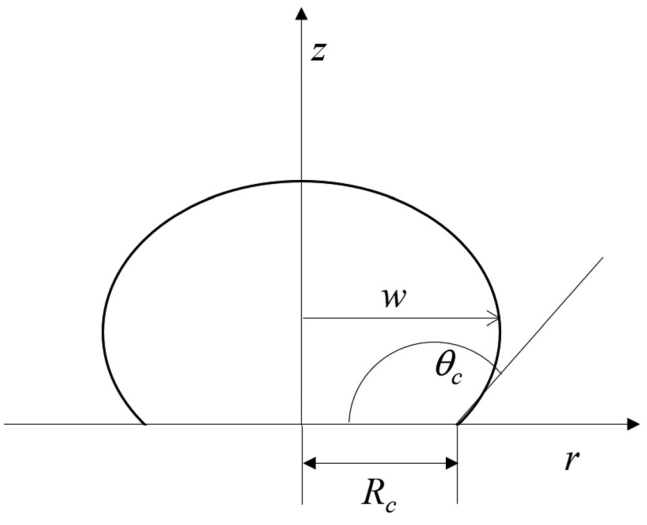

FIG. 1. Schematic of a deformed sessile drop.

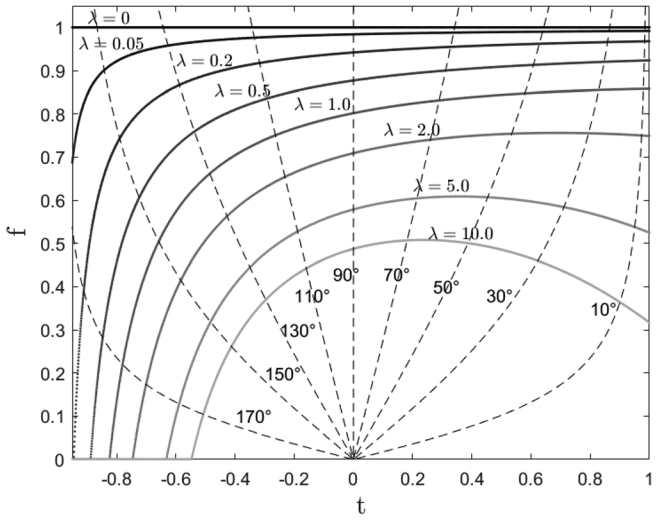

FIG. 2. Dashed curves are iso-θ_c, and they define the values of t_0 for each λ, through the intersection with the solid curves.

external convection, it is nil everywhere. When the gas mixture thermophysical properties are assumed constant, as for almost all the available analytical models for sessile drop evaporation, Eq. (7) yields

$$N_j^{(T)} = cD_{10}\nabla_j H, \tag{9}$$

where $N_j^{(T)} = N_j^{(0)} + N_j^{(1)} = N_j^{(1)}$, and $H = \ln(1 - y^{(1)})$, and since $\nabla_j N_j^{(T)} = 0$, the Laplace equation for the potential H is obtained,

$$\nabla^2 H = 0. \tag{10}$$

Introducing the Dirichlet boundary condition at drop surface and at infinity as

$$y^{(1)} = y_s^{(1)} \text{ on the drop surface,} \tag{11}$$

$$y^{(1)} = y_\infty^{(1)} \text{ at infinity,} \tag{12}$$

and introducing the auxiliary function $\Phi = \frac{H - H_\infty}{H_s - H_\infty}$, we can see that the function Φ satisfies the harmonic problem,

$$\nabla^2 \Phi = 0, \tag{13a}$$

$$\Phi_s = 1; \quad \Phi_\infty = 0. \tag{13b}$$

In Ref. 6, it was shown that assuming some simplified, but generally accepted, dependence of the gas mixture thermophysical properties on the temperature, the solution of the vapor diffusion problem set by Eq. (8) and the heat diffusion into the gas mixture, taking into account the Stefan flow, can be analytically described for generally shaped drop shapes once the auxiliary function Φ is known.

Section III focuses on solving the problem (10) for the case of a deformed sessile drop. The results can then be extended to the most general case, following Ref. 6, as done in Ref. 5, for instance.

III. NUMERICAL APPROACH: DESCRIPTION, METHODS, AND TESTS

The species conservation equations (8) were numerically solved using the commercial code COMSOL Multiphysics, which implements a finite element discretization approach. The auxiliary function Φ [Eq. (13)] is evaluated on 2D numerical axis-symmetric grids, whose sizes are set proportional to the drop equivalent radius, R_{eq} (i.e., the radius of the spherical drop having the same volume of the selected drop). This is a compromise between the desirable grid refinement and the imposition of appropriate uniform conditions at the free stream. For the simulations shown here, the outer radius of the computation domain, R_∞, is set equal to 30 drop radii, and Fig. 3 illustrates this. The Dirichlet uniform conditions at the boundaries [see Eq. (13b)] corresponding to the drop surface and the free stream (see Fig. 3) are imposed as follows: on the drop surface, the auxiliary function Φ is set equal to 1, while on the spherical boundary, representing the free stream the Dirichlet condition, is set following an iterative procedure. The value of $\Phi_{R=R_\infty}$ is set equal to

$$\Phi'_\infty = -(\nabla_R \Phi)_{R=R_\infty} R_\infty, \tag{14}$$

and the value of the gradient $(\nabla_R \Phi)_{R=R_\infty}$ is calculated from the previous solution. The iteration terminates when the differences between two subsequent values of Φ'_∞ are lower than 10^{-5}. The value of $R_\infty = 30R_{eq}$ was chosen as a reasonable compromise between the desirable grid refinement and the approximate uniform boundary

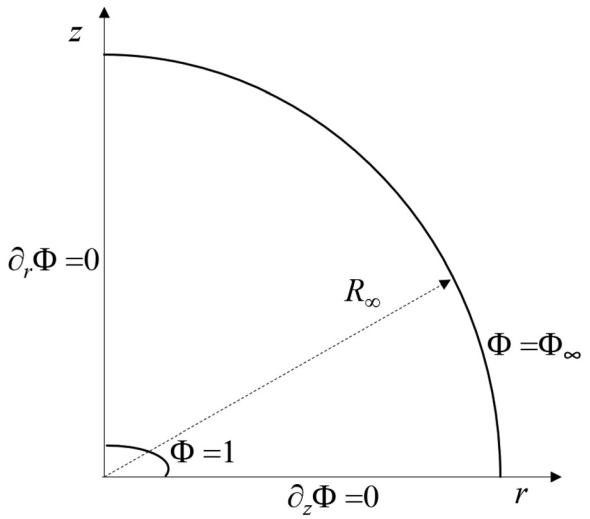

FIG. 3. Schematic of the computational domain.

conditions at the free stream. The iterative procedure described above assures that the choice of R_∞ has a negligible effect on the calculation accuracy. More details of this procedure and relative tests are described in Ref. 20.

One of the main outcomes of the numerical simulations is the evaporation rate, which is evaluated by integrating the vapor mass fluxes on a spherical surface that contains the boundary corresponding to the drop surface (see again Fig. 3). This procedure is necessary for drops on a hydrophilic substrate to overcome the well-known issue (see, for example, Ref. 3) of the flux diverging at the triple line. In addition, it generally minimizes the numerical errors that arise when evaluating the fluxes on a grid boundary.

Previous grid independence analysis[5,20] using 2D axis-symmetric and 3D computational meshes up to 10^5 and 10^6 elements, respectively, on test cases with spherical cap sessile drops, for which exact analytical solutions exist, had shown a discrepancy between the evaporation rates predicted by the numerical approach and the exact analytical solutions consistently lower than 10^{-4} for sessile drops on hydrophobic substrates and lower than 10^{-3} for sessile drops on hydrophilic substrates.

The computational meshes used for the present investigation are made by 2D axis-symmetric grids with approximately 5×10^4 triangular elements.

A. Test cases

The effect of the drop deformation due to gravity on the drop evaporation rate is evaluated for sessile drops on various hydrophilic and hydrophobic substrates and different drop volumes. The drop contact angle varied from 40° up to 150°, which covers a wide range of real-life conditions,[21] and the degree of drop deformation due to the increased drop volume in the gravitational field, which is defined by the Bond number $Bo = \frac{\rho g R_{eq}^2}{\sigma}$, where R_{eq} is the volume equivalent radius [i.e., the radius of the spherical drop having the same volume of the selected drop, $R_{eq} = \left(\frac{3V}{4\pi}\right)^{1/3}$], ranged between 0.1 (almost spherical

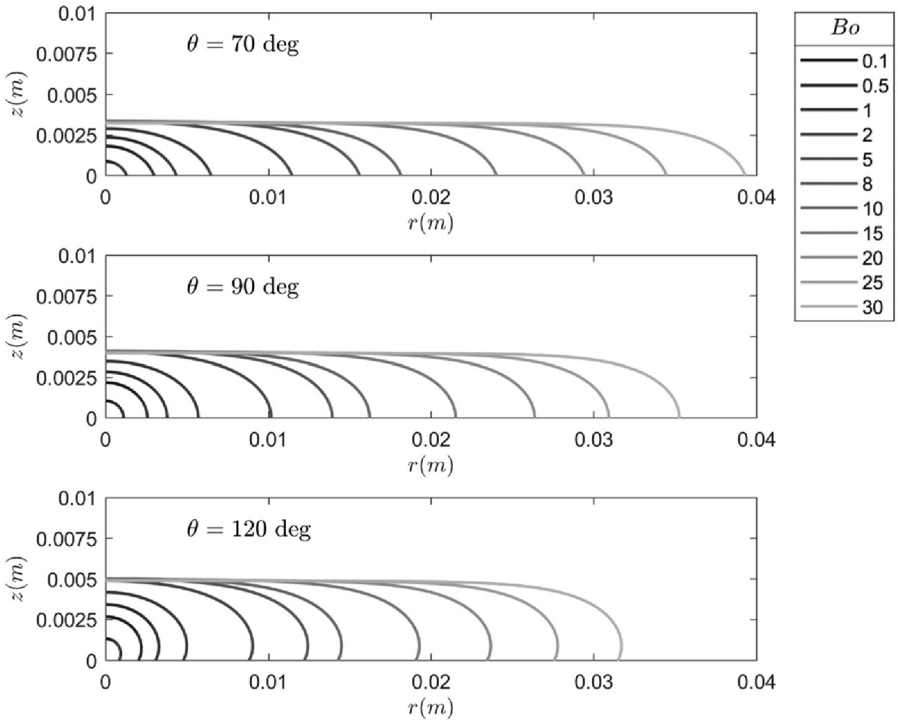

FIG. 4. Drop profiles for the full range of *Bo* and three θ_c (see Table I). Water drops in the terrestrial gravitational field.

drop) and 30 (highly deformed drop). Figure 4 shows an example of the drop shape for different contact angles and drop volumes, as obtained from the above-described solution.

The 12 values of the contact angle θ_c and the 11 values of the Bond number *Bo* selected for the present investigation are reported in Table I, for a total number of test cases equal to 132. Since the drop equivalent radius increases with *Bo*, the radius of the spherical surface corresponding to the free stream conditions, which is set equal to 30 R_{eq}, increases as well, and the corresponding mesh is reshaped for each case.

The range of the Bond number corresponds to water drop volumes in the terrestrial gravitational field ranging from 2.7 μl (for $Bo = 0.1$) to 14.0 ml (for $Bo = 30$).

IV. RESULTS AND DISCUSSION

The evaporation rate from a drop deformed by gravity differs from that of a drop in the absence of the gravitational field, since the drop shape is different, and the aim of the present investigation is to quantify this effect. It is usually assumed that when the drop size is smaller than the capillary length $[L_c = (\frac{\sigma}{\rho g})^{1/2}]$, the drop shape can be safely assumed to be a spherical cap, and an analytical solution in toroidal coordinates[4] can be used to evaluate the vapor fluxes on the surface and, ultimately, the evaporation rate. On this basis, Picknett and Bexon[8] derived a polynomial correlation to account for the effect of wall wettability (i.e., the value of the contact angle θ_c) on the drop evaporation rate. However, when the drop equivalent radius increases, the effect of gravity may produce large deformations (see Fig. 4). Consequently, the evaporation rate varies with respect to the spherical shape case. It is worth noting that for a drop already having an equivalent radius equal to the capillary length (i.e., $Bo = 1$), the deviation from the spherical shape is evident, as shown in Fig. 5, where the actual drop shape is compared to that in the absence of gravity for three different contact angles.

TABLE I. Values of the contact angle θ_c and the Bond number *Bo* investigated.

$\theta_c(^\circ)$	40, 50, 60, 70, 80, 90, 100, 110, 120, 130, 140, 150
Bo(-)	0.1, 0.5, 1.0, 2,0, 5.0, 8.0, 10.0, 15.0, 20.0, 25.0, 30.0

The effect of drop deformation due to gravity on the evaporation rate can be summarized by introducing the non-dimensional parameter *G*, defined as the ratio between the evaporation rate from the deformed drop and the evaporation rate from the spherical cap (non-deformed drop) with the same volume and the same contact angle,

$$G(Bo, \theta_c) = \frac{m_{ev}(R_{eq}, \theta_c, Bo)}{m_{ev}(R_{eq}, \theta_c, 0)}. \quad (15)$$

The quantity on the numerator, $m_{ev}(R_{eq}, \theta_c, Bo)$, is found by the numerical solution described above (with an accuracy between 10^{-3} and 10^{-4}) and the quantity in the denominator is calculated by the Picknett and Bexon correlation.[8] The above-mentioned numerical solution of the field equation allowed one to quantify the effect, and Fig. 6 shows the parameter *G* as a function of the Bond number *Bo*, for all the 12 selected contact angles, corresponding to hydrophilic and hydrophobic configurations.

The graph shows that under hydrophilic conditions, the non-dimensional quantity *G* monotonically increases with the increase in drop size (i.e., increase in deformation) with respect to the case with no gravity effect (spherical cap drop). All the test cases under

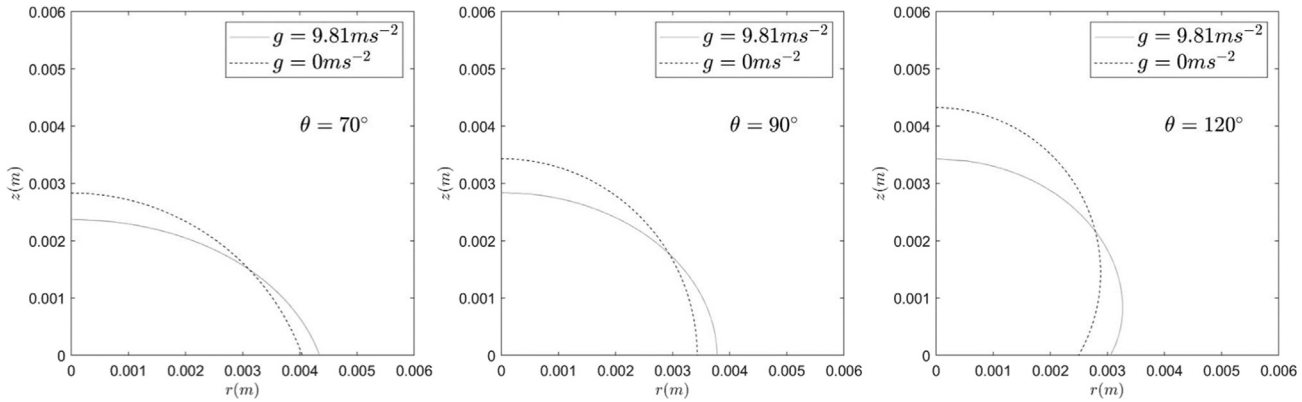

FIG. 5. Drop surface profiles for $Bo = 1$ (solid line) and profiles of spherical caps with the same volume (dashed lines); water drops in the terrestrial gravitational field.

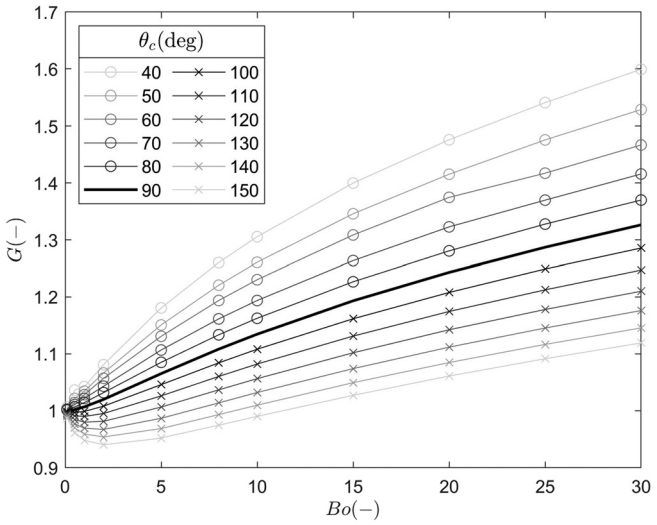

FIG. 6. Profiles of the non-dimensional parameter G as a function of *Bo* and θ_c.

hydrophobic conditions show a different behavior of the function *G*: For small deformations, *G* diminishes, reaching a relative minimum corresponding to a value of *Bo* that depends on θ_c, and then increases for larger deformations. The values of the Bond number where $G = 1$ is recovered are reported in Table II, for all the hydrophobic test cases considered. The value of *Bo* corresponding to the minimum of the function $G(Bo, \theta_c)$ increases with the increasing contact angle.

It should also be noted that by fixing the value of the Bond number *Bo*, *G* decreases, thus increasing the contact angle.

TABLE II. Values of Bond number *Bo* where $G = 1$ is recovered for the selected hydrophobic test cases.

θ_c (°)	100	110	120	130	140	150
$Bo_{(G=1)}$	1.15	2.48	4.25	6.49	8.84	11.36

The following is a possible qualitative explanation for different evaporation behaviors of sessile drops under hydrophilic and hydrophobic substrates subject to gravity: For drops with contact angles lower than 90° (i.e., on a hydrophilic substrate), the larger the drop deformation, the larger the drop surface exposed to the gas (see Fig. 7) and this may explain the monotonic increase in the evaporation rate with size. On the other hand, for drops on hydrophobic substrates, that is, θ_c greater than 90°, the drop deformation due to gravity has a double effect on its evaporation behavior. For small deformations, the increase in the drop deformation corresponds to the decrease in the drop exposure to the gaseous flow, with an initial decrease on the drop surface (see Fig. 7). Conversely, it leads to an increase in the drop Gaussian curvature in the region close to the triple line (see Fig. 8) corresponding to higher evaporation fluxes (i.e., higher evaporation rate).

It should be noted that the apparently counter-intuitive decrease in the drop surface does not mean a decrease in the total interfacial energy since the corresponding increase in the base radius over-

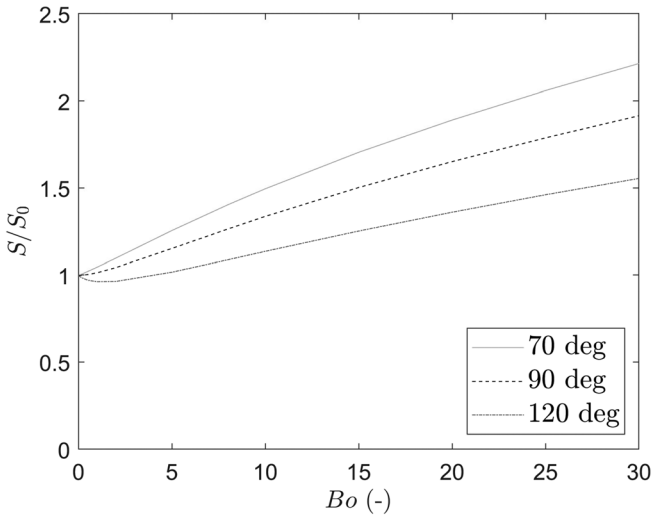

FIG. 7. Ratio between the deformed drop surface and the surface of an equal volume spherical cap for the full range of *Bo* and three θ_c (see Table I).

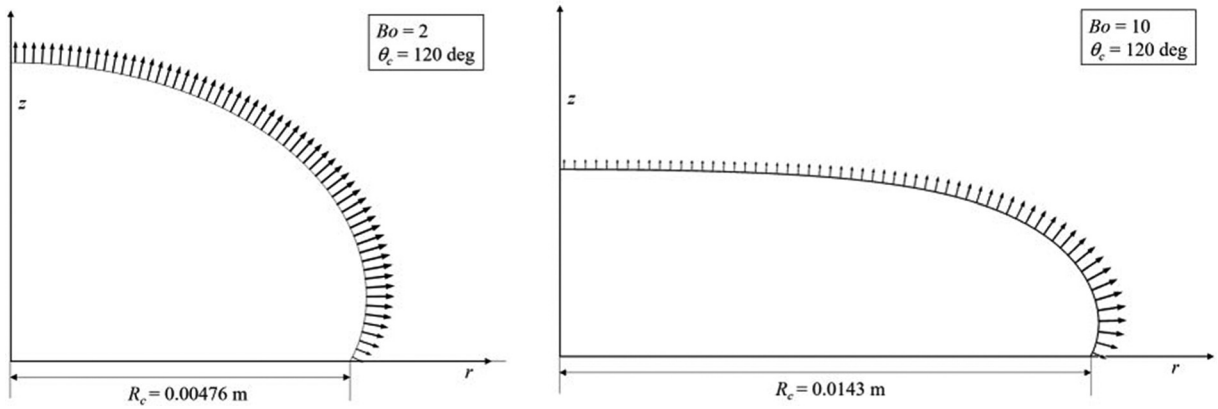

FIG. 8. Vapor fluxes over the surface of sessile drops with $Bo = 2$ (left) and $Bo = 10$ (right) on a hydrophobic substrate with $\theta_c = 120°$ (figure scaling is given by the drop base radius).

compensate (for the hydrophobic case) the decrease in the liquid–gas interfacial energy.

Evidence of the qualitative explanation reported above can be seen in Fig. 8, which shows the vapor fluxes on the drop surface of two sessile drops on a hydrophobic substrate with a contact angle equal to 120°, deformed by gravity for $Bo = 2$ and $Bo = 10$. The graphs qualitatively show that the increase in the drop deformation reduces the uniformity of the drop surface curvature with respect to the spherical cap shape, and the vapor fluxes are higher in the region corresponding to the higher curvature. In previous works, it was shown that the Gaussian curvature, rather than the mean curvature, affects the evaporation fluxes. Furthermore, a perfect proportionality between vapor flux and Gaussian curvature was shown to exist for the special case of spheroidal and triaxial ellipsoidal-shaped drops.[22]

This result cannot be applied to the present case, but an effect of the Gaussian curvature can be observed as follows. Quantitative evidence is shown in Fig. 9, reporting the profiles (circles) of the non-dimensional vapor fluxes, defined as

$$\hat{n}_{ev} = \frac{n_n^{(1)} 4\pi R_{eq}^2}{m_{ev}}, \tag{16}$$

where $n_n^{(1)} = Mm^{(1)} N_n^{(1)}$ and plotted as a function of the polar angle ϕ, for three values of Bo (0.1, 1, 10) and for $\theta_c = 90°$. The graph also shows the profiles (solid lines) of the non-dimensional Gaussian curvature K_G^* along the drop surface for each of the selected test cases, defined as

$$K_G^* = \sqrt{2}\left(K_G R_{eq}^2\right)^{\frac{1}{4}}, \tag{17}$$

where K_G is the Gaussian curvature on the drop surface (refer to the Appendix for the details).

The graph shows a correlation between the non-dimensional flux and the Gaussian curvature: For highly deformed drops, the Gaussian curvature increases approaching the triple line (increasing ϕ), and correspondingly the vapor flux increases too; the effect is more clearly seen in the increasing drop deformation (higher Bo).

Figure 10 illustrates the correlation between the non-dimensional vapor fluxes and the non-dimensional Gaussian curvatures along the drop surface for three contact angles equal to 70°, 90°, and 120°, corresponding to three substrate conditions, and for all the 11 values of the Bond number Bo investigated (refer to Table I). The graphs confirm that there exists a range of K_G^* close to 1 where the vapor fluxes can be reasonably well correlated with the Gaussian curvature; the large deviation in the proximity of the triple line is related to the fact that the vapor flux on the triple line on a hydrophobic substrate must become nil, while it diverges for the case of hydrophilic substrates (see, for example, Ref. 3).

With the aim of providing a simple tool to calculate the correction to the evaporation rate of drops deformed by gravity, a correlation for the parameter G as a function of the drop contact angle θ_c and the Bond number Bo has been derived for sessile drops vaporizing on hydrophobic or hydrophilic substrates.

In the case of a contact angle θ_c higher than 90° (hydrophobic substrates), using a trial and error approach, the following three-

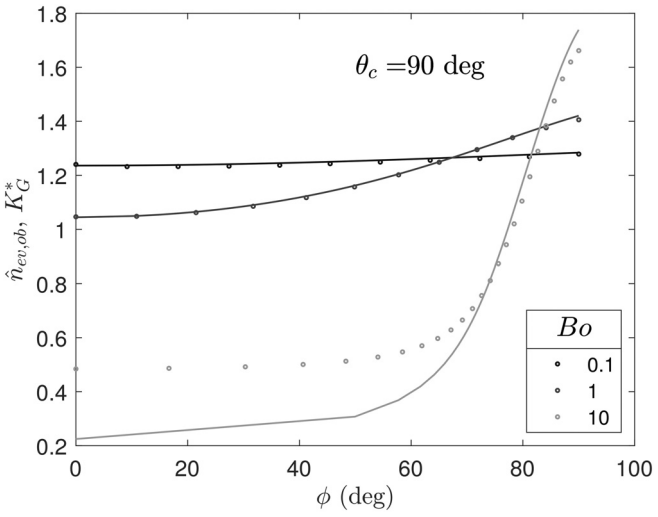

FIG. 9. Non-dimensional vapor flux and non-dimensional Gaussian curvature as a function of the polar angle ϕ (see the box in the figure), for three Bond numbers and a contact angle of 90°.

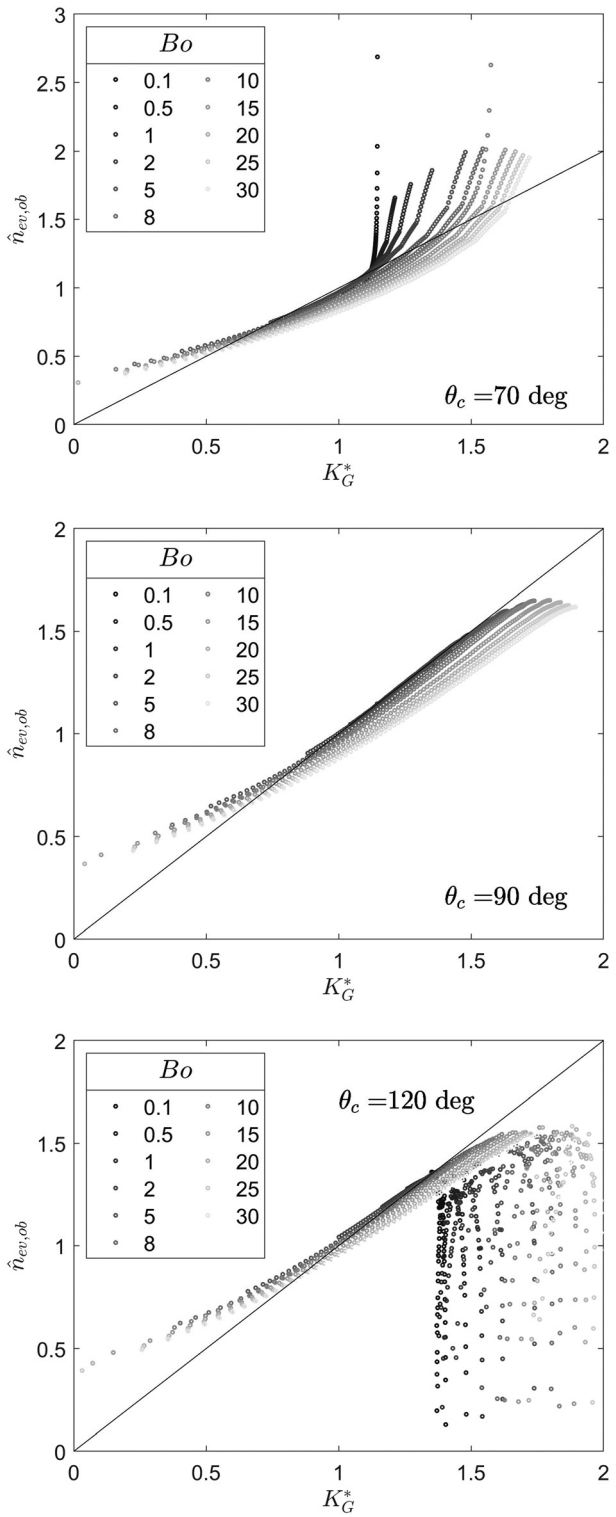

FIG. 10. Correlation between the non-dimensional vapor flux and non-dimensional Gaussian curvature over the drop surface for the full range of *Bo* and three θ_c (see Table I).

parameter correlation was chosen, since it was found to be suitable in accounting for the particular shape of the function $G(\theta_c, Bo)$,

$$G(\theta_c, Bo) = 1 - C_0\left(\frac{y}{1+y}\right) + C_1 \log(1+y), \tag{18}$$

$$y = \frac{Bo}{C_2(\theta_c)}, \tag{19}$$

where the coefficients $C_j(\theta_c)$ are evaluated by fitting the data with first- and second-order polynomial functions of the contact angle θ_c, that is

$$C_n(\theta) = \sum_{k=0}^{m_n} a_k^n \theta_c^k, \tag{20}$$

with

	$n=0$	$n=1$	$n=2$
m_n	1	2	2
a_0^n	2.377	6.037×10^{-1}	14.812
a_1^n	-1.06×10^{-2}	-4.334×10^{-3}	-1.384×10^{-1}
a_2^n	⋯	9.436×10^{-6}	3.587×10^{-4}

In the case of hydrophilic substrates, a third-order polynomial correlation is proposed as

$$G(\theta_c, Bo) = \sum_{j=0}^{3} D_n(\theta) Bo^n, \tag{21}$$

where the numerical coefficients, which are functions of the contact angle, are defined as

$$D_n(\theta) = \sum_{k=0}^{m_n} b_k^n \theta_c^k, \tag{22}$$

with

	$n=0$	$n=1$	$n=2$	$n=3$
m_n	2	1	1	1
b_0^n	1.008	5.925×10^{-2}	-1.857×10^{-3}	2.603×10^{-5}
b_1^n	-2.519×10^{-5}	-5.097×10^{-4}	1.996×10^{-5}	-3.041×10^{-7}
b_2^n	-1.514×10^{-6}	⋯	⋯	⋯

The maximum discrepancy between the results from the numerical solution and the proposed correlations is less than 0.8% for the hydrophobic substrates and less than 1.05% for the hydrophilic substrates; the average discrepancy was found to be better than 0.25% for the hydrophobic substrates and better than 0.37% for the hydrophilic substrates.

These correlations allow a relatively simple extension of the Picknett–Bexon correlation[8] for evaluating the evaporation rate of sessile drops to the cases of non-negligible deformations due to the effect of gravity.

V. CONCLUSIONS

Evaporation of sessile drops on flat hydrophilic and hydrophobic substrates was analyzed to systematically quantify the effect of drop deformation due to gravity. The deviation from the spherical cap shape, which is assumed by sessile drops in the absence of gravity, is measured by the Bond number based on the equivalent drop radius, and values of *Bo* up to 30 (highly deformed drops) are considered, while the contact angle was assumed to be in the range between 40°and 150°.

A numerical solution to the Laplace equation was used to quantify the vapor fluxes and the evaporation rates. The drop deformation was found to affect the evaporation differently for the cases of hydrophilic and hydrophobic substrates. As a general observation, for highly deformed drops, the increase in the local Gaussian curvature in the region toward the drop borders was found to drive the increment of the evaporation rate with respect to the drop in the absence of gravity. For large deformations ($Bo = 30$), the increase in evaporation rates ranges from 10% to 60%, but also for $Bo = 1$ (usually taken as a safe condition for the assumption of a spherical cap shape), deviations up to 5% may be found as a function of the contact angle.

Thanks to the systematic analysis, the quantitative results are used to propose two simple correlations to correct the evaporation rates found from the Picknett–Bexon correlation, as a function of size (*Bo* number) and contact angle. The correlations were found to be different for hydrophobic and hydrophilic surfaces. They were able to approximate the functional dependence, with an average deviation of less than 0.37%.

AUTHOR DECLARATIONS

Conflict of Interest

The authors have no conflicts to disclose.

Author Contributions

Simona Tonini: Conceptualization (equal); Data curation (equal); Formal analysis (equal); Methodology (equal); Software (equal); Writing – original draft (equal); Writing – review & editing (equal). **Gianpietro E. Cossali:** Conceptualization (equal); Data curation (equal); Formal analysis (equal); Investigation (equal); Methodology (equal); Software (equal); Writing – original draft (equal); Writing – review & editing (equal).

DATA AVAILABILITY

The data that support the findings of this study are available from the corresponding author upon reasonable request.

APPENDIX: NON-DIMENSIONAL FLUX VS NON-DIMENSIONAL CURVATURES FOR AN OBLATE SPHEROIDAL CAP

Consider a free oblate drop, whose equivalent radius is

$$R_{eq,ob} = \left(\frac{3V_{ob}}{4\pi}\right)^{\frac{1}{3}}, \tag{A1}$$

the non-dimensional vapor flux on the drop surface is defined as

$$\hat{n}_{ev,ob} = \frac{n_{ev,ob}4\pi R_{eq,ob}^2}{m_{ev,ob}}, \tag{A2}$$

and its relation with the Gaussian curvature is[22]

$$\hat{n}_{ev,ob} = \frac{n_{ev,ob}4\pi R_{eq,ob}^2}{m_{ev,ob}} = \left(K_G R_{eq,ob}^2\right)^{\frac{1}{4}}. \tag{A3}$$

The shape of a sessile drop with a contact angle of 90° and small values of Bond number *Bo* can be approximated by that of half of an oblate drop (see, for example, Ref. 19), and its equivalent radius is

$$R_{eq,ses} = \left(\frac{3V_{ses}}{4\pi}\right)^{\frac{1}{3}}, \tag{A4}$$

where V_{ses} is the drop volume, which is half of the volume of an oblate free drop, V_{obl}, with the same semi-axes: $V_{ses} = \frac{V_{ob}}{2}$. The relationship between the equivalent radius of the free oblate drop, $R_{eq,obl}$, and that of the sessile drop is then

$$R_{eq,ob} = \left(\frac{3 \times 2V_{ses}}{4\pi}\right)^{\frac{1}{3}} = 2^{\frac{1}{3}} R_{eq,ses}. \tag{A5}$$

For the particular case of a contact angle of $\theta_c = 90°$, the evaporation rate of the sessile drop is equal to half of that of the corresponding free drop. Then, $m_{ev,ses} = \frac{m_{ev,ob}}{2}$, while the vapor fluxes on the drop surfaces are the same, $n_{ev,ses} = n_{ev,ob}$.

From Eq. (A3), eliminating from the LHS the quantities relative to the oblate free drop-in favor of those relative to the sessile drop yields

$$\hat{n}_{ev,ob} = \frac{n_{ev,ob}4\pi R_{eq,ob}^2}{m_{ev,ob}} = \frac{n_{ev,ses}4\pi 2^{\frac{2}{3}} R_{eq,ses}^2}{2m_{ev,ses}} = 2^{-\frac{1}{3}} \frac{n_{ev,ses}4\pi R_{eq,ses}^2}{m_{ev,ses}}, \tag{A6}$$

whereas the RHS becomes

$$\left(K_G R_{eq,ob}^2\right)^{\frac{1}{4}} = \left(K_G 2^{\frac{2}{3}} R_{eq,ses}^2\right)^{\frac{1}{4}} = 2^{\frac{1}{6}} \left(K_G R_{eq,ses}^2\right)^{\frac{1}{4}}. \tag{A7}$$

Using the same definition of the non-dimensional vapor flux, $\hat{n}_{ev,ses} = \frac{n_{ev,ses}4\pi R_{eq,ses}^2}{m_{ev,ses}}$, Eq. (A3) can be rewritten as

$$\hat{n}_{ev,s} = \frac{n_{ev,s}4\pi R_{eq,ses}^2}{m_{ev,ses}} = \sqrt{2}\left(K_G R_{eq,ses}^2\right)^{\frac{1}{4}} = K_G^*. \tag{A8}$$

This relationship holds only for the case described here (oblate drop with $\theta_c = 90°$), but it is used in the text as a tool to understand the evaporation behavior of deformed sessile drops.

REFERENCES

[1]H. Y. Erbil, "Evaporation of pure liquid sessile and spherical suspended drops: A review," Adv. Colloid Interface Sci. **170**(1–2), 67–86 (2012).
[2]P. Gurrala, S. Balusamy, S. Banerjee, and K. C. Sahu, "A review on the evaporation dynamics of sessile drops of binary mixtures: Challenges and opportunities," Fluid Dyn. Mater. Process. **17**(2), 253–284 (2021).
[3]S. K. Wilson and H. M. D'Ambrosio, "Evaporation of sessile droplets," Annu. Rev. Fluid Mech. **55**, 481–509 (2023).

[4]N. N. Lebedev, *Special Functions & Their Applications* (Dover Publications, 1972).
[5]G. E. Cossali and S. Tonini, "Analytical solutions for modelling the evaporation of sessile drops," Appl. Math. Modell. **114**, 61–77 (2023).
[6]G. E. Cossali and S. Tonini, "An analytical model of heat and mass transfer from liquid drops with temperature dependence of gas thermo-physical properties," Int. J. Heat Mass Transfer **138**, 1166–1177 (2019).
[7]S. S. Sazhin, *Droplets and Sprays: Simple Models of Complex Processes* (Springer Nature, 2022).
[8]R. G. Picknett and R. Bexon, "The evaporation of sessile or pendant drops in still air," J. Colloid Interface Sci. **61**(2), 336–350 (1977).
[9]F. Bashforth and J. C. Adams, *An Attempt to Test the Theories of Capillary Action* (Cambridge Press, 1883).
[10]W. M. Robertson and G. W. Lehman, "The shape of a sessile drop," J. Appl. Phys. **39**(4), 1994–1996 (1968).
[11]G. E. Wang and J. J. Lannutti, "Static wetting of a liquid drop on a solid," J. Mater. Sci. **30**, 3171–3176 (1995).
[12]E. Bormashenko and G. Whyman, "Variational approach to wetting problems: Calculation of a shape of sessile liquid drop deposited on a solid substrate in external field," Chem. Phys. Lett. **463**, 103–105 (2008).
[13]P. Dhar, R. K. Dwivedi, and A. R. Harikrishnan, "Surface declination governed asymmetric sessile droplet evaporation," Phys. Fluids **32**(11), 112010 (2020).
[14]J. De Coninck, J. C. Fernández-Toledano, F. Dunlop, T. Huillet, and A. Sodji, "Shape of pendent droplets under a tilted surface," Physica D **415**, 132765 (2021).
[15]P. Jia, M. Zhou, H. Yu, C. Lv, and G. Jing, "Local evaporation flux of deformed liquid drops," arXiv:2108.07588 (2021).
[16]P. J. Sáenz, K. Sefiane, J. Kim, O. K. Matar, and P. Valluri, "Evaporation of sessile drops: A three-dimensional approach," J. Fluid Mech. **772**, 705–739 (2015).
[17]W. Cui, Y. Cao, S. Wang, T. Zhang, H. Ma, C. Chang, D. Liang, and J. Dong, "Numerical study on the evaporation of a non-spherical sessile droplet," Micromachines **14**(1), 76 (2023).
[18]M. L. Timm, E. Dehdashti, A. Jarrahi Darban, and H. Masoud, "Evaporation of a sessile droplet on a slope," Sci. Rep. **9**(1), 19803 (2019).
[19]H. Y. Erbil and R. A. Meric, "Evaporation of sessile drops on polymer surfaces: Ellipsoidal cap geometry," J. Phys. Chem. B **101**, 6867–6873 (1997).
[20]S. Tonini and G. E. Cossali, "Analytical modeling of the evaporation of sessile drop linear arrays," Phys. Rev. E **105**(5), 054803 (2022).
[21]V. Pachchigar, M. Ranjan, and S. Mukherjee, "Role of hierarchical protrusions in water repellent superhydrophobic PTFE surface produced by low energy ion beam irradiation," Sci. Rep. **9**(1), 8675 (2019).
[22]S. Tonini and G. E. Cossali, "One-dimensional analytical approach to modelling evaporation and heating of deformed drops," Int. J. Heat Mass Transfer **97**, 301–307 (2016).